Available online at www.sciencedirect.com
SCIENCE DIRECT®
Journal of Solid State Chemistry 177 (2004) 2550–2556
JOURNAL OF SOLID STATE CHEMISTRY
http://elsevier.com/locate/jssc

Synthesis, structure and magnetic properties of $Na_6Co_2O_6$

M. Sofin, E.-M. Peters, and M. Jansen*

Max-Planck-Institut für Festkörperforschung, Heisenbergstrasse 1, D-70569 Stuttgart, Germany

Received 22 December 2003; received in revised form 25 March 2004; accepted 28 March 2004

Abstract

$Na_6Co_2O_6$ was synthesized via the azide/nitrate route by reaction between NaN_3, $NaNO_3$ and Co_3O_4. Stoichiometric mixtures of the starting materials were heated in a special regime up to 500°C and annealed at this temperature for 50 h in silver crucibles. Single crystals have been grown by subsequent annealing of the reaction product at 500°C for 500 h in silver crucibles, which were sealed in glass ampoules under dried Ar. According to the X-ray analysis of the crystal structure ($P\bar{1}$, $Z = 1$, $a = 5.7345(3)$, $b = 5.8903(3)$, $c = 6.3503(3)$ Å, $\alpha = 64.538(2)$, $\beta = 89.279(2)$, $\gamma = 85.233(2)°$, 1006 independent reflections, $R_1 = 8.34\%$ (all data)), cobalt is tetrahedrally coordinated by oxygen. Each two CoO_4 tetrahedra are linked through a common edge forming $Co_2O_6^{6-}$ anions. Cobalt ions within the dimers, being in a high spin state ($S = 2$), are ferromagnetically coupled ($J = 17\,cm^{-1}$). An intercluster spin exchange ($zJ' = -4.8\,cm^{-1}$) plays a significant role below 150 K and leads to an antiferromagnetically ordered state below 30 K. Heat capacity exhibits a λ-type anomaly at this temperature and yields a value of 19.5 J/mol K for the transition entropy, which is in good agreement with the theoretical value calculated for the ordering of the ferromagnetic-coupled dimers. In order to construct a model for the spin interactions in $Na_6Co_2O_6$, the magnetic properties of Na_5CoO_4 have been measured. This compound features isolated CoO_4 tetrahedra and shows a Curie–Weiss behavior ($\mu = 5.14\,\mu_B$, $\Theta = -20$ K) down to 15 K. An antiferromagmetic ordering is observed in this compound below 10 K.

Keywords: Azide/nitrate route; Sodium cobalt oxide; Crystal structure; Magnetic properties; Heat capacity

1. Introduction

It is well known that cobalt exhibits mainly oxidation states +2 and +3 in its compounds, for which a huge number of representatives are known [1]. Very few compounds contain cobalt in any of the other valences. The alkali metal oxocobaltates are special in that, plenty of cobaltates(II) are known [2–5], but only a few ternary oxides with alkali metals containing Co^{III} were synthesized so far [6–9]. Moreover, the number of known oxocobaltates(III) and (IV) [10–14] are approximately the same, although the latter are regarded as a really unusual valence for cobalt. A possible reason behind this finding might be the peculiarities of solid-state synthesis normally used for obtaining such compounds. Running the preparation under oxygen atmosphere or using peroxides (hyperoxides) as starting materials leads to oxocobaltates(IV), when high alkali metal/cobalt ratios (>1) are used. A direct synthesis from the binary compounds (as is feasible in the case of oxoferrates(III)) is not possible, because no pure and stable cobalt(III) oxide is available.

The known alkali oxocobaltates(III) can be divided into two groups with the general formulas A_5CoO_4 and $ACoO_2$ (A = alkali metal). The structures of compounds from the first group (Na_5CoO_4 [8], $Li_3Na_2CoO_4$ [9]) consist of isolated CoO_4 tetrahedra. Compounds from the latter group have structures depending on the sizes of the alkali metal cation. With small ions (Li [15,16], Na [6,17]) distorted CoO_6 octahedra sharing through faces build up layers, which are separated by the layers of alkali cations. The anions of cobaltates with heavier alkali metals [7,18] adopt the cristobalite structure with the tetrahedral environment of cobalt. An exception here is α-$KCoO_2$ [18], in which cobalt has a square-pyramidal coordination by oxygen.

Although the magnetic properties of the Co^{III}, in general, are well investigated [19], only few reports are to be found in the literature on the magnetism of the

*Corresponding author. Fax: +49-711-689-1502.
E-mail address: m.jansen@fkf.mpg.de (M. Jansen).

0022-4596/$ - see front matter © 2004 Published by Elsevier Inc.
doi:10.1016/j.jssc.2004.03.036

alkali metal oxocobaltates(III). To our knowledge, only $NaCoO_2$ showing temperature-independent paramagnetism due to the low spin state in the octahedral arrangement has been studied [6].

In this work we present a new sodium oxocobaltate(III), which features interesting structural and physical properties. Its structure is characterized by a novel $Co_2O_6^{6-}$ anion consisting of two edge-sharing CoO_4 tetrahedra. Since $Na_6Co_2O_6$ shows a rather complicated magnetic behavior, the magnetic properties of Na_5CoO_4 [8] have also been investigated for reference. The structure of the latter cobaltate is built up from isolated CoO_4 tetrahedra. Thus its magnetic behavior can be used as a starting point for interpretation of the magnetism of $Na_6Co_2O_6$.

Both cobaltates(III) were synthesized using a new, recently developed approach [20], which allows to circumvent difficulties of the conventional solid-state synthesis from the binary oxides. Here, we demonstrate by another examples, how versatile this route is, especially at adjusting the oxygen content in the target compounds. Thus pure products can be achieved, which is absolutely necessary for a reliable investigation of physical properties, in particular, of the magnetic behavior.

2. Experimental

$Na_6Co_2O_6$ and Na_5CoO_4 were obtained via the azide/nitrate route [20]. Starting materials for the preparation of the sodium cobaltates were NaN_3 (Sigma-Aldrich, 99.5%), $NaNO_3$ (Aldrich, 99%) and Co_3O_4. Cobalt oxide was prepared by heating $Co(C_2O_4)\cdot 2H_2O$ (Johnson Matthey, 99%) in a flow of oxygen at 350°C for 20 h. The starting materials were mixed in the ratio required according to Eqs. (1) and (2) and ground in a ball mill, pressed in pellets ($\varnothing$ 13 mm) under 10^5 N, dried under vacuum (10^{-2} mBar) at 150°C for 12 h and placed under argon in a tightly closed steel vessel (for its design cf. Ref. [5]), provided with a silver inlay. In a flow of dry argon, the following temperature profile was applied: 25→260°C (100°C/h); 260→380°C (5°C/h), 380→500°C (20°C/h) and subsequent annealing for 50 h at 500°C.

$$44NaN_3 + 10NaNO_3 + 6Co_3O_4 = 9Na_6Co_2O_6 + 71N_2, \quad (1)$$

$$74NaN_3 + 16NaNO_3 + 6Co_3O_4 = 18Na_5CoO_4 + 119N_2. \quad (2)$$

The obtained dark red ($Na_6Co_2O_6$)/red (Na_5CoO_4) powders, being extremely sensitive to humid air, were sealed in glass ampoules under argon atmosphere and all following manipulations with these substances were performed in inert atmospheres of purified argon.

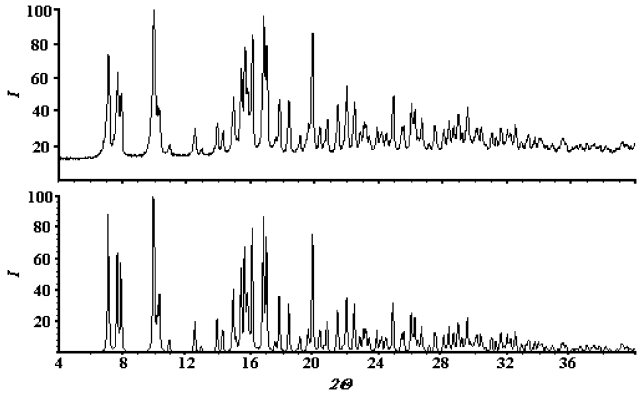

Fig. 1. Measured XRD pattern of $Na_6Co_2O_6$ (above) and calculated from single-crystal data (below).

Hazards: the temperature control, as given above, must be strictly followed. Rapid heating or running the reaction in a closed (sealed) ampoule can lead to dangerous explosion.

Single crystals of $Na_6Co_2O_6$ have been grown by subsequent annealing of the pressed reaction product at 500°C for 500 h in silver crucibles, which were sealed in glass ampoules under dried Ar.

The X-ray investigation on powder samples was performed on an STOE StadiP diffractometer with Mo$K\alpha_1$ radiation ($\lambda = 0.709300$ Å) at room temperature using a position-sensitive detector and a curved germanium monochromator. The powder diffraction data were collected in the range of 4–40° in 2Θ. The collected powder data for $Na_6Co_2O_6$ are given in Fig. 1. The single-crystal diffraction data were collected on an STOE three-cycle diffractometer equipped with a CCD detector at 293 K.

Thermal analyses of $Na_6Co_2O_6$ were carried out using a DTA/TG device (STA 409, Netzsch) coupled with a quadrupole mass spectrometer (QMG 421, Balzers). The probe was heated at a rate of 10°C/min in a corundum crucible under dry argon. Heat capacity was measured on a PPMS device (Quantum Design).

Magnetic measurements were performed on a SQUID-Magnetometer (MPMS 5.5, Quantum Design) between 5 and 330 K in magnetic fields up to 5 T. The diamagnetic correction has been applied using tabulated values [21].

3. Results and discussion

$Na_6Co_2O_6$ can be easily prepared by the azide/nitrate route as a micro-crystalline powder. The dark red product obtained is very sensitive to moisture. According to DTA/TG the substance starts melting at ~670°C, which is accompanied by a decomposition resulting in $NaCoO_2$ [6,17], the only solid phase detectable by X-ray diffraction in the solid residue.

Na_5CoO_4 has been obtained in the same way as $Na_6Co_2O_6$. The red powder is also very sensitive to moisture. X-ray diffraction was used to check the purity of the product by comparing the measured pattern with the calculated one from the known structure [8].

The crystal structure of the new sodium cobaltate $Na_6Co_2O_6$ was determined from single-crystal data collected at 293 K. For the details and results of the structure refinement, see Tables 1–3. Interatomic distances, coordination numbers, effective coordination numbers and mean fictive ionic radii [22] for $Na_6Co_2O_6$ are given in Table 4.

According to the single-crystal structure analysis, cobalt is coordinated tetrahedrally by oxygen. This is a relatively rare situation for Co^{III}, but one can find a few representatives containing Co^{III} in a tetrahedral coordination in the literature (e.g., Na_5CoO_4 [8], $Li_3Na_2CoO_4$ [9]). The prominent structural feature in $Na_6Co_2O_6$ is the novel $Co_2O_6^{6-}$ ion (Fig. 2) consisting of two edge-sharing CoO_4 tetrahedra. The Co–O bond lengths (Table 4) agree, on average, well with the data reported in the literature [8,9]. Considering the Co–O–separations in detail, one notices significant variances, reflecting strong disturbance of the ideal geometry of the tetrahedra. However, this can be easily understood in terms of the different functionalities of the oxygen atoms involved. The centering Co^{III} cations of one Co_2O_6 dimer repel each other, which results in elongated Co–O bonds to the bridging ligands (1.96, 1.97 Å for Co–O2), and in a contraction of the corresponding angle, 86° for O2–Co–O2. As a consequence, the bond lengths to the terminal oxygen atoms are shorter (1.79 Å for Co–O1 and Co–O3) and the corresponding angle is much above the ideal tetrahedral value of 109° (here 124° for O1–Co–O3). The sodium atoms are coordinated by five (Na1 and Na3), or four (Na2), oxygen atoms in the form of distorted tetragonal pyramids and a tetrahedron, respectively. The Na–O distances vary from 2.28 to 2.59 Å (Table 4), which is in the expected range. The Co_2O_6 units are stacked along the *a*-axis (Fig. 3). As a whole, the structure can be considered a very distorted hcp of oxygen atoms with Co and Na2 in tetrahedral and Na1 and Na3 in square-pyramidal coordinations (displacement from octahedral sites due to the strong distortion). Although this compound is a 3D structure, it can be imagined as "layers" consisting of polyhedra around sodium and cobalt taken together, and stacked along [100]. Then Co and Na3 as well as Na1 and Na2, respectively, accommodate a similar occupation pattern of the respective cation sites for each "layer" perpendicular to [100]. It is interesting to note that the Co_2O_6 unit consisting of two edge-sharing $Co^{III}O_4$ tetrahedra has already been observed as a part of an oligomeric $Co_4O_{10}^{10-}$ anion [23]. In spite of similar ionic radii, $Na_6Co_2O_6$ is not isostructural to Na_3FeO_3 [24]. The structure of the sodium ferrate is characterized by infinite chains consisting of corner-sharing FeO_4 tetrahedra. In contrast, $K_6Fe_2O_6$ [25] shows Fe_2O_6 dimers in analogy to $Na_6Co_2O_6$.

The magnetic susceptibilities of $Na_6Co_2O_6$ and Na_5CoO_4 have been measured on powder samples between 5 and 330 K and for magnetic fields ranging from 0.1 to 5 T. The susceptibilities, which were

Table 1
X-ray and crystallographic data for $Na_6Co_2O_6$ (293 K)

Crystal data	
Crystal system	Triclinic
Space group, Z	$P\bar{1}$ (No. 2), 1
Lattice constants (from powder/single crystal), Å and deg	$a = 5.736(1)/5.734(2)$ $b = 5.890(1)/5.888(2)$ $c = 6.350(1)/6.346(3)$ $\alpha = 64.54(1)/64.52(4)$ $\beta = 89.28(1)/89.24(3)$ $\gamma = 85.23(1)/85.23(3)$
Molar mass (g/mol)	351.8
Molar volume (cm^3/mol)	58.03
Calculated density (g/cm^3)	3.03
Crystal shape, color	Irregular, dark red
Crystal size (mm)	$0.1 \times 0.1 \times 0.1$
Structure determination	
Structure solution	Direct methods, SHELXS-97 [29]
Structure refinement	Full-matrix least-squares on F^2, SHELXL-97 [29]
Parameters refined	64
$R_1(F_o > 4\text{sig}\, F_o^2/\text{all})$	0.0473/0.0834
wR_2	0.0689
Weight w	$w = 1/(\sigma^2(F_o^2) + (0.0099 \cdot P)^2$, $P = (\max(F_o^2, 0) + 2 \cdot F_c^2)/3$
$\Delta\rho_{min}/\rho_{max}$, $e^-/Å^3$	–0.98/0.78
Data collection	
Diffractometer	STOE CCD
Monochromator	Graphite
Wavelength (Å)	Mo$K\alpha$, 0.71073
2Θ range for data collection	$2\Theta < 73.38$
$h\,k\,l$-range	$-7 < h < 8, -7 < k < 9, -9 < l < 9$
Absorption correction	SADABS [30]
Total no. reflection	1791
Unique reflections	1006
Absorption coefficient. μ (mm^{-1})	4.62
$F(000)$	168

Table 2
Atomic coordinates for $Na_6Co_2O_6$

Atom	Site	x	y	z
Co	*2i*	0.3590(1)	0.1907(1)	0.3115(1)
Na1	*2i*	0.0629(3)	0.7683(4)	0.4444(3)
Na2	*2i*	0.8556(3)	0.2345(4)	0.0237(3)
Na3	*2i*	0.4366(3)	0.2585(4)	0.7445(3)
O1	*2i*	0.2460(5)	0.1008(6)	0.0995(5)
O2	*2i*	0.3075(5)	0.9230(6)	0.6242(5)
O3	*2i*	0.2556(5)	0.4700(6)	0.3429(5)

Table 3
Anisotropic thermal displacement parameters[a] (in Å^2) for $Na_6Co_2O_6$

Atom	U_{11}	U_{22}	U_{33}	U_{23}	U_{13}	U_{12}
Co	0.0119(3)	0.0140(4)	0.0123(3)	–0.0065(3)	0.0012(2)	–0.0017(3)
Na1	0.0147(10)	0.0199(11)	0.0227(11)	–0.0122(9)	0.0044(8)	–0.0037(9)
Na2	0.0183(11)	0.0301(13)	0.0130(10)	–0.0062(9)	0.0018(8)	–0.0003(9)
Na3	0.0163(10)	0.0224(11)	0.0173(10)	–0.0090(9)	0.0035(8)	–0.0060(9)
O1	0.0122(17)	0.0202(19)	0.0131(16)	–0.0094(15)	0.0010(13)	–0.0038(14)
O2	0.0125(17)	0.0148(18)	0.0117(16)	–0.0018(14)	0.0026(13)	–0.0038(14)
O3	0.0127(17)	0.0131(17)	0.0176(18)	–0.0086(14)	0.0024(13)	–0.0020(14)

[a] Defined as: $\exp[-2\pi^2(a^{*2}h^2U_{11} + b^{*2}k^2U_{22} + c^{*2}l^2U_{33} + 2b^*c^*klU_{23} + 2a^*c^*hlU_{13} + 2a^*b^*hkU_{12})]$.

Table 4
Interatomic distances (in Å), coordination numbers (CN), effective coordination numbers (ECoN) and mean fictive ionic radii (MEFIR) [18] for $Na_6Co_2O_6$

Atom	O1	O2	O3	CN	EcoN	MEFIR
Co	1.790(1)	1.960(1) 1.971(1)	1.792(1)	4	3.7	0.40
Na1	2.515(1)	2.290(1) 2.589(1)	2.313(1) 2.421(1)	5	4.6	0.93
Na2	2.295(1) 2.526(1)	2.245(1)	2.285(1)	4	3.7	0.87
Na3	2.333(1) 2.524(1)	2.567(1)	2.379(1) 2.500(1)	5	4.8	0.98
CN	6	6	6			
ECoN	5.6	5.5	5.9			
MEFIR	1.46	1.48	1.44			

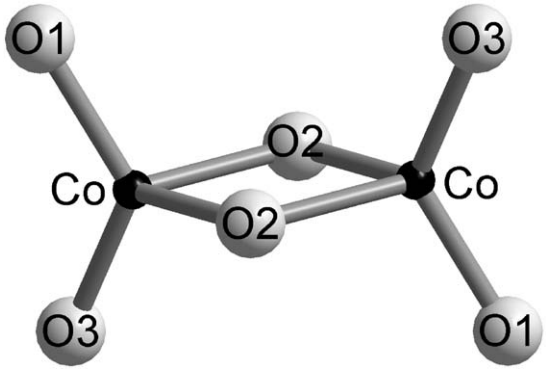

Fig. 2. Structure of the $Co_2O_6^{6-}$ anion.

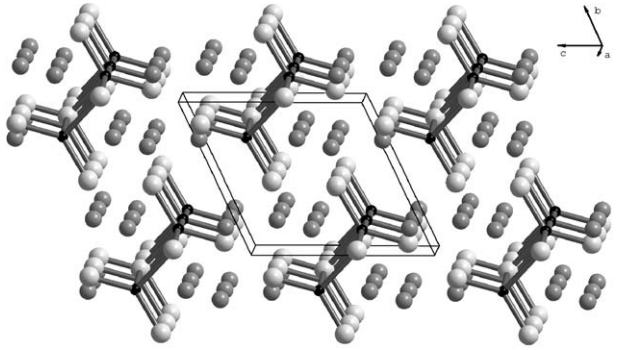

Fig. 3. Perspective view of the crystal structure of $Na_6Co_2O_6$ (Co—black, Na—grey, O—white balls).

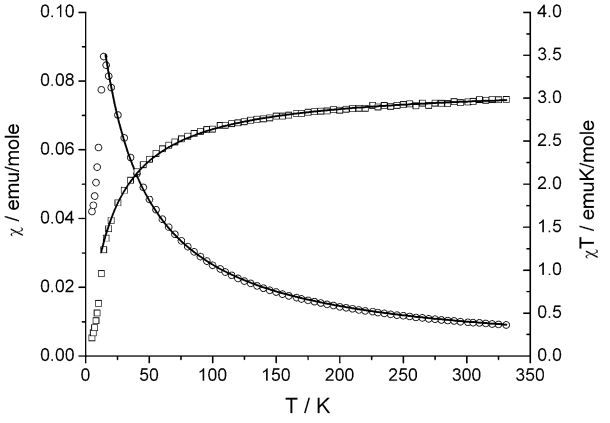

Fig. 4. Magnetic susceptibility of Na_5CoO_4 represented as χ vs. T (circles) and $\chi \cdot T$ vs. T (squares). The full line corresponds to the fit using Eq. (3).

independent of the magnetic field strength, are displayed in Fig. 4 (Na_5CoO_4) and Fig. 5 ($Na_6Co_2O_6$) for $H = 1$ T.

The magnetic susceptibility of Na_5CoO_4 can be adequately described in the range 15–330 K by the Curie–Weiss law (Eq. 3), assuming $S = 2$. The resulting fit (parameters obtained: $g = 2.10$, $\Theta = -20$ K) is shown in Fig. 4 as solid lines. We have preferred to show the magnetic properties of Na_5CoO_4 (Fig. 4) as $\chi(T)$ and $\chi T(T)$ curves, instead of a $\chi^{-1}(T)$ representation, because of a better comparability with the magnetism of $Na_6Co_2O_6$, for which a $\chi^{-1}(T)$ graph is not representative. However, for Na_5CoO_4 one would see a straight line in the $\chi^{-1}(T)$ depiction.

$$\chi = \frac{N_A\mu_B^2 g^2}{3k_B(T-\Theta)}S(S+1). \quad (3)$$

The abrupt decrease of the susceptibility of Na_5CoO_4 below 10 K indicates an onset of antiferromagnetic order, which would be already expected from the

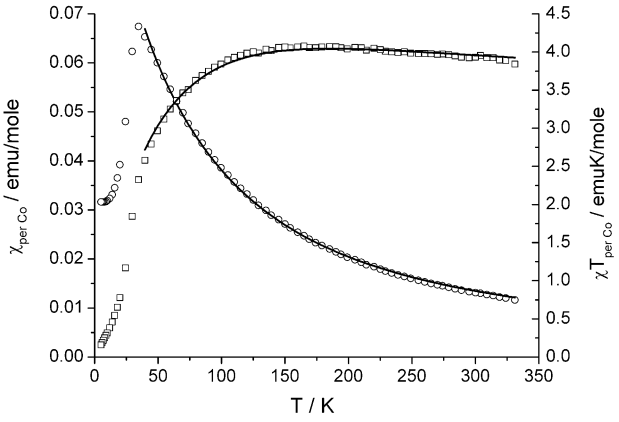

Fig. 5. Magnetic susceptibility of $Na_6Co_2O_6$ represented as χ vs. T (circles) and $\chi \cdot T$ vs. T (squares). The full line corresponds to the fit using Eq. (6).

negative value of the paramagnetic Curie temperature Θ. From the magnetism of Na_5CoO_4 one can conclude that Co^{III} in a tetrahedral oxocoordination features a rather simple magnetic behavior. The cobalt ions are in a high spin state and have a temperature-independent magnetic moment. An unquenched spin–orbit coupling gives rise to the observed g value which, however, remains constant at cooling to at least 15 K. The drop in the effective magnetic moment (expressed as χT in Fig. 4) is due to spin interaction between cobalt ions. The interaction strength can be evaluated from Θ according to Eq. (4): $zJ' = -0.4\,cm^{-1}$. Below 10 K, the antiferromagnetic spin interaction is sufficiently strong to align the spins antiparallel in the ordered state. A Curie–Weiss behavior for Co^{III} ions in the tetrahedral sites was also observed in the mixed-valent cobaltate $Na_9Co_2O_7$ [26], but the value of the magnetic moment for Co^{III} could not be evaluated unequivocally from the susceptibility data because of the presence of Co^{II} ions.

$$\Theta = 2S(S+1)zJ'/3k_B. \quad (4)$$

The most visible difference from the magnetic behavior of $Na_6Co_2O_6$ (Fig. 5) is the significantly higher χT values (given per one Co ion) compared to Na_5CoO_4 (Fig. 4). Moreover, in the case of $Na_6Co_2O_6$ these values are slightly increasing with decreasing temperature, to a maximum at about 175 K. For Na_5CoO_4 χT values are continuously decreasing with temperature. Nevertheless, both compounds show an antiferromagnetic ordering at low temperatures as can be seen from $\chi(T)$ curves. The effective magnetic moment in $Na_6Co_2O_6$ obtained for one cobalt at 300 K ($\mu_{eff} = (3\chi k_B T/N_A)^{1/2}$) is equal to 5.52 μ_B, which exceeds significantly the spin-only value (4.90 μ_B), and is on the upper limit of the expected range for a d^6 ion [19]. On the basis of the magnetic behavior of Na_5CoO_4 (supposing that for Co^{III} in tetrahedral oxocoordination: the zero-field splitting effect is negligible at given temperatures and the spin–orbit coupling can be considered by an increased, but constant g factor), we assumed that the rather high effective magnetic moment and its increase with dropping temperature arise from a ferromagnetic coupling between Co^{III} ions within the Co_2O_6 cluster. At further cooling, after this coupling has reached the saturated state, the intercluster exchange, which is antiferromagnetic, becomes significant and leads to the continuous decrease of χT values below 150 K. Since the intercluster exchange is three dimensional, it causes finally an antiferromagetically ordered state as observed below 30 K (cf. the $\partial\chi/\partial T$ curve). The specific heat (Fig. 6) shows a λ-type anomaly at this temperature. In general, such a type of χT curve is characteristic of substances having spin interactions of different nature. Thus, here one can also imagine antiferromagnetically coupled dimers with a ferromagnetic interdimer interaction. However in a given case, one would expect a field dependence in the susceptibility below the ordering temperature, which is not observed. Moreover, the local spin exchange should be stronger, as one can deduce from the Co–Co separations. Thus, for the antiferromagnetic intradimer interaction, one cannot expect such a high value of the effective magnetic moment. Furthermore, the geometry of the Co_2O_6 anion is giving support to assuming the ferromagnetic interaction within dimer, because of the Co–O–O angle lying close to 90°. Finally, the heat capacity measurements strongly support the point of view for the ferromagnetically coupled cobalt ions in the dimers (see below).

In order to obtain the coupling strength within the dimer, a Heisenberg model for pairs of coupled spins ($S_1 = S_2 = 2$) has been used: $\hat{H}_{ex} = -2J\hat{S}_1\hat{S}_2$ (resulting in Eq. (5)). Only a poor fit and unrealistic parameter values were obtained using Eq. (5), indicating that

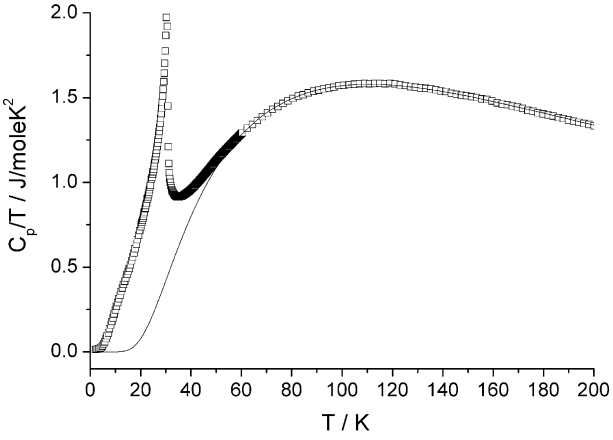

Fig. 6. C_p/T vs. T (squares) and calculated lattice contribution (full line) by Einstein model (see text) for $Na_6Co_2O_6$.

interdimer exchange interactions are not negligible in this case. To also take into account the interdimer exchange interaction, significantly affecting the susceptibility already below 150 K, a new parameter had to be included. For the case $|J| \gg |zJ'|$, it would be sufficient to include a Θ term in Eq. (5). However, we have not succeeded in obtaining a satisfactory fit using this approach. Thus, the experimental data were fitted using Eq. (6), containing the J' term introducing the intercluster exchange interaction in a more complicated way [27]

$$\chi_{\mathrm{perCo}} = \frac{N_A \mu_B^2 g^2}{k_B T} F(J,T) = \frac{N_A \mu_B^2 g^2}{k_B T} \frac{e^{2x} + 5e^{6x} + 14e^{12x} + 30e^{20x}}{1 + 3e^{2x} + 5e^{6x} + 7e^{12x} + 9e^{20x}}, \quad (5)$$

where $x = J/k_B T$

$$\chi_{\mathrm{perCo}} = \frac{N_A \mu_B^2 g^2}{k_B T - 2zJ' F(J,T)} F(J,T), \quad (6)$$

here z is the number of nearest neighbors. In an idealized structure of $Na_6Co_2O_6$ ($a \approx b \approx c$, $\beta \approx \gamma \approx 90°$, $\alpha \approx 60°$), and assuming the Co_2O_6 units as points, one can take $z = 8$. The eight next neighbors can be easily seen in Fig. 3: six in the bc plane, one above and one below this plane. A least-squares fit of the χT data using Eq. 6 between 40 and 330 K yields $J = 17\,\mathrm{cm}^{-1}$, $zJ' = -4.8\,\mathrm{cm}^{-1}$, $g = 2.11$, and the full lines in Fig. 5. The parameter values obtained are in full agreement with the qualitative discussion above. Anisotropy, which is expected to be important for Co^{III} in distorted tetrahedral coordination, does not significantly affect the magnetic properties above 40 K. The ferromagnetic nature of intradimer interaction can be attributed, as already mentioned, to the Co–O–Co angle lying close to 90° [28]. The fitted g-factor in $Na_6Co_2O_6$ (2.11) is found to be very close to the one in Na_5CoO_4 (2.10), which supports our suggestion of a similarity in the magnetic behavior of cobalt ions in these compounds (neglecting interspin interaction). The intercluster interactions are significantly different for $Na_6Co_2O_6$ ($zJ' = -4.8\,\mathrm{cm}^{-1}$) and Na_5CoO_4 ($zJ' = -0.4\,\mathrm{cm}^{-1}$), which is also reflected in the ordering temperatures (30 K for $Na_6Co_2O_6$ and 10 K for Na_5CoO_4). This could be attributed to a better separation of the cobaltate anions by sodium cations in Na_5CoO_4 (the Na/Co ratio is equal to 3 for $Na_6Co_2O_6$ and 5 for Na_5CoO_4). In the previously published data on the magnetic behavior of $Na_{10}Co_4O_{10}$ [23] containing Co^{III} ions in a virtually identical surrounding, the g factor was found to be 2.15, which is again in good agreement with the results for $Na_6Co_2O_6$. Moreover, the magnetic analysis of the $Na_{10}Co_4O_{10}$ behavior was based on the assumption that in the Co_4O_{10} cluster the coupling between the terminal Co^{II} and the next Co^{III} ions is stronger than the interaction between the central Co^{III} ions. The Co^{III}–Co^{III} coupling could not be quantified from the magnetic data of $Na_{10}Co_4O_{10}$. However, as established in this work, the Co^{III}–Co^{III} interaction ($17\,\mathrm{cm}^{-1}$) is, as supposed, significantly weaker than that for Co^{II}–Co^{III} ($-40.5\,\mathrm{cm}^{-1}$) in $Na_{10}Co_4O_{10}$ [23]; however, it is not negligible.

The specific heat of $Na_6Co_2O_6$ was measured between 2 and 300 K (Fig. 6). The curve exhibits a λ-type anomaly at 30 K, which correlates very well with the magnetic ordering as observed in the susceptibility curves. In order to calculate an entropy change associated with the phase transition, one should first subtract the lattice contribution to the total specific heat. Since no isomorphic nonmagnetic compound is available, it is necessary to extrapolate the lattice specific heat from the temperature range where it dominates to the range of the phase transition. The $C_p(T)$ dependences at low temperatures is well matched by a cubic term βT^3. However, the value of β cannot be used for the determination of the Debye temperature, since both the phonon and magnetic subsystems of the antiferromagnet give cubic terms in the specific heat at low temperatures. Moreover, the fitting of the specific heat by the Debye model at high temperatures is questionable, because the Debye temperature for $Na_6Co_2O_6$, as in many real materials, is rather strongly temperature dependent. Thus, the fitting of the lattice specific heat was performed between 60 and 200 K by the Einstein model using three modes. The extrapolation of the calculated curve ($\Theta_{E1} = 172$ K, $\Theta_{E2} = 328$ K, $\Theta_{E3} = 546$ K) to lower temperatures allows for the subtraction of the lattice contribution. The experimental $C_p(T)/T$ curve as well as the curve obtained from the fitting procedure are shown in Fig. 6. The numerical integration of the $C_{mag}(T)/T$ between 2 and 60 K gives the value of the magnetic entropy ΔS_{mag} released on the ordering of magnetic subsystem. For calculating an expected value for the entropy change, one should keep in mind that the remaining magnetic entropy reflects the thermal population of the energy levels of the dimer. At 30 K one obtains: 99.9% for $S_{dimer} = 4$, 0.01% for $S_{dimer} = 3$, and other levels are negligibly low populated. The experimental value of ΔS_{mag} obtained (19.5 J/mol K) is close to the expected value (18.3 J/mol K). The excess entropy change may be attributed to the underestimation of the lattice specific heat by using the Einstein model. About 75% of entropy is released below the Neel temperature.

Acknowledgments

We thank J. Nuss for collecting X-ray single-crystal data, E. Brücher for the measurement of magnetic properties as well as G. Siegle for providing the specific heat measurement.

References

[1] A.F. Holleman, E. Wiberg, N. Wiberg, Lehrbuch der Anorganischen Chemie, Walter de Gruyter, Berlin-New York, 1995.
[2] M.G. Barker, G.A. Fairhall, J. Chem. Res. S (1979) 371.
[3] W. Burow, R. Hoppe, Z. Anorg. Allg. Chem. 467 (1980) 158.
[4] F. Bernhardt, R. Hoppe, Z. Anorg. Allg. Chem. 620 (1994) 586.
[5] M. Sofin, E.-M. Peters, M. Jansen, Z. Anorg. Allg. Chem. 628 (2002) 2697.
[6] M. Jansen, R. Hoppe, Z. Anorg. Allg. Chem. 408 (1974) 104.
[7] C. Delmas, C. Fouassier, P. Hagenmuller, J. Solid State Chem. 13 (1975) 165.
[8] W. Burow, R. Hoppe, Naturwissenschaften 67 (1980) 192.
[9] J. Birx, R. Hoppe, Z. Anorg. Allg. Chem. 597 (1991) 19.
[10] M. Jansen, Z. Anorg. Allg. Chem. 417 (1975) 35.
[11] M. Jansen, R. Hoppe, Z. Anorg. Allg. Chem. 398 (1973) 54.
[12] R. Olazcuaga, J.M. Reau, M. Devalette, G.L. Flem, P. Hagenmuller, J. Solid State Chem. 13 (1975) 275.
[13] M. Jansen, R. Hoppe, Z. Anorg. Allg. Chem. 409 (1974) 152.
[14] M. Jansen, R. Hoppe, Z. Anorg. Allg. Chem. 408 (1974) 75.
[15] H.J. Orman, P.J. Wiseman, Acta Crystallogr. C 40 (1984) 12.
[16] R.J. Gummow, M.M. Thackeray, W.I.F. David, S. Hull, Mater. Res. Bull. 27 (1992) 327.
[17] C. Fouassier, G. Matejka, J.M. Reau, P. Hagenmuller, J. Solid State Chem. 6 (1973) 532.
[18] M. Jansen, R. Hoppe, Z. Anorg. Allg. Chem. 417 (1975) 31.
[19] H. Lueken, Magnetochemie, Teubner, Stuttgart-Leipzig, 1999.
[20] D. Trinschek, M. Jansen, Angew, Chem. Int. Ed. Engl. 38 (1999) 133.
[21] Landolt-Börnstein Handbook, Zahlenwerte und Funktionen aus Naturwissenschaften und Technik; Neue Serie, Gr. II, Bd. 2, Springer, Berlin, 1966.
[22] R. Hoppe, Z. Kristallogr. 150 (1979) 23.
[23] M. Sofin, H.-U. Güdel, R. Bircher, E.-M. Peters, M. Jansen, Angew. Chem. Int. Ed. Engl. 42 (2003) 3527.
[24] B.M. Sobotka, A. Möller, Z. Anorg. Allg. Chem. 629 (2003) 2063.
[25] H. Rieck, R. Hoppe, Z. Anorg. Allg. Chem. 408 (1974) 151.
[26] M. Sofin, E.-M. Peters, M. Jansen, Solid State Sci. 6 (2004) 339.
[27] A.P. Ginsberg, M.E. Lines, Inorg. Chem. 11 (1972) 2289.
[28] J.B. Goodenough, Magnetism and the Chemical Bond, Wiley, New York, 1963.
[29] G.M. Sheldrick, University of Göttingen, Göttingen, 1997.
[30] G.M. Sheldrick, SADABS, Bruker AXS, Inc., Madison, WI, 1998.